Active vibration damping of bladed structures

A. Paknejad [1], G. Raze [2], G. Zhao [1], A. Deraemaeker [3], G. Kerschen [2], C. Collette [1,2]
[1] Université Libre de Bruxelles, BEAMS Department,
Av. F.D Roosevelt 50, 1050 Brussels, Belgium

[2] Université de Liège, Aerospace and Mechanical Engineering Department,
Allée de la Découverte 9, 4000 Liège, Belgium

[3] Université Libre de Bruxelles, BATir Department,
Av. F.D Roosevelt 50, 1050 Brussels, Belgium

Abstract
This paper investigates the potential of using an active control system to mitigate broadband vibrations of bladed structures. Piezoelectric patches are used for both sensing the motion and actuating the control force. To maximize control authority, the size and location of piezoelectric patches are optimized based on maximizing the strain energy. Two new designs of active control law, which are inspired by force-feedback configuration, are developed for the plant having alternating pole-zero pairs in the frequency response function (FRF). Numerical simulations are performed to assess the performance of the designed control system in terms of the closed-loop damping of the system with high modal density. The parameters of the control law are tuned based on maximizing the minimum damping of the first family of modes. Experimental tests are performed to validate the numerical design.

1 Introduction

Bladed assemblies are widely used in aerospace applications and in particular turbomachinery structures. New technologies have been developed to improve the performance of the system in terms of the energy consumption by using low-density structures. These structures, however, possess a very low internal damping which may lead to high-cycle fatigue problem and malfunctions. Suppressing their vibration is of interest for many researchers and engineers in this field. There are two common methods for reducing vibrations i.e. passive and active.

Passive control systems are simply integrated to the structures with no need of external power sources and additional hardware for their operations. Friction damping devices [1–4] and piezoelectric shunt damping [5–9] are two passive techniques which have been used to damp the vibration of the bladed assemblies. Friction damping devices dissipate energy when a relative motion occur between the structure and the device [1]. Although this can be used as an effective vibration absorber, its performance is difficult to assess since friction is a nonlinear phenomenon [2–4]. Piezoelectric patches connected to an electrical network known as shunt damping is another passive technique to mitigate the vibration of bladed structures. Basically, the piezoelectric effect transforms mechanical energy into electrical energy which is dissipated through the electrical network [10]. Schwarzendahl et al. [5] implemented this technique on a bladed structure and optimized the parameters of the shunt to minimize the amplitude of the first mode. Mokrani et al. [6] tuned the shunt elements using the average frequency of the first bending modes family. It should be noted that the performance of the controlled system is basically dependent on the electromechanical coupling factor [11]. Therefore, the use of active control system in order to improve the control authority of the piezoelectric shunt damping was studied on the bladed structures as well. Kauffman et al. [7] proposed a semi-active approach using low-power frequency-switching. The use of negative capacitance was proposed in [11] and implemented on a test-rig of a bladed disk model with eight blades [8]. Note that the negative capacitance is an active electrical device. Tang et al. [9] implemented an active-passive-hybrid-piezoelectric-network (known as APPN), which was first introduced by Agnes [12], on a rotationally periodic structure. Basically, APPN integrates piezoelectric shunt damping with an active voltage or charge source to improve the performance of the system.

Active control systems were introduced to overcome the performance limitations of the passive methods since they are less sensitive to the system's parameters [13]. These approaches require an integration of sensors, actuators and control units to artificially increase the total damping in the systems. A special attention to the use of piezoelectric transducers has been given in active control methods since they can be used as both sensors as well as actuators and it is easy to integrate them on the fan rotor-stator [14], the composite fan blades [15], rotor blades [16]. Although effective, the piezoelectric transducers were placed directly on the blades where the strain energy is maximized. In practice, locating the transducers on the blades may lead to an important perturbation in the aerodynamic flow.

When piezoelectric sensor and actuator are collocated, the open-loop transfer function contains alternating pole-zero configuration which has no high frequency roll-off. Depending on the strain distribution of a mode at the location of the piezoelectric patches, the zero of the open-loop transfer function may appear either after or before the pole, which is an important key in the design of the active control system. When the zero comes after pole, positive-position-feedback (PPF) is proposed as an interesting active control law. Although it amplifies the static response which may lead to a decrease in the stiffness of the structure, the controller adds the high-frequency roll-off. PPF can be implemented by using a first- or a second-order filter. The second-order PPF is a resonant control which outperforms the first-order PPF in terms of the damping ratio of the system; however, its performance degrades rapidly under the resonance uncertainty in comparison to that of the first-order PPF. This technique was implemented on a cantilever beam when its parameters were optimized based on the method of maximum damping [17] and H_∞ optimization [18]. In case the zero goes before the pole, the open-loop transfer function is similar to the system when a force actuator is collocated to a force sensor. For such systems, integral-feedback (IF) [19] and α-controller [20], which includes a simple integrator and a double integrator combined with a real zero in the feedback loop, respectively, were introduced as effective control laws. It was shown that α-controller provides a better control performance in comparison to IF although it is less robust to resonant uncertainty. Consequently, the control law can be inspired by IF and/or α-controller if the zero of the open-loop transfer function from the piezoelectric actuator to the piezoelectric sensor appear before pole.

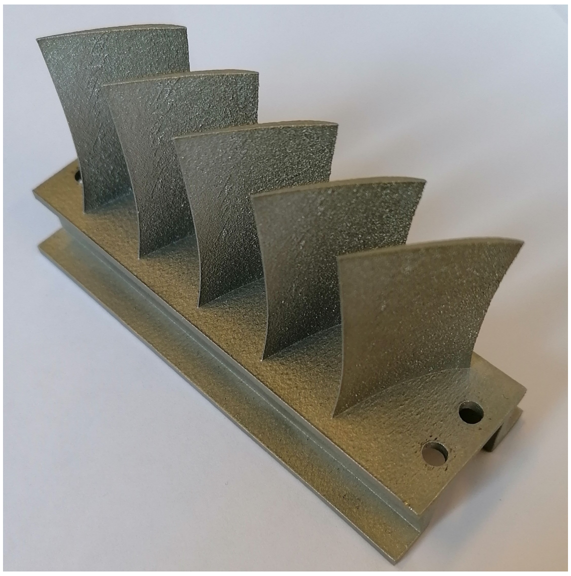

Figure 1: The bladed rail

This paper studies the potential of using an active control system to damp the vibration of a bladed rail structure. A numerical modeling of the system is discussed in details. This includes the dynamic behavior

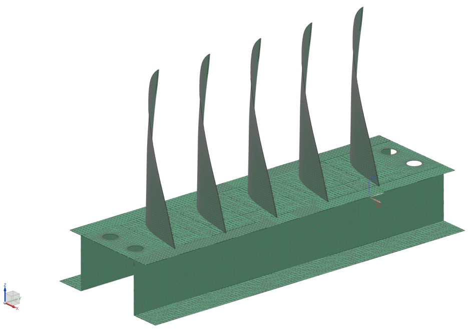

(a)

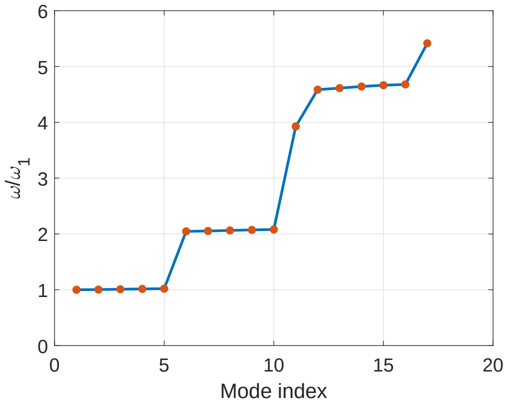

(b)

Figure 2: (a) Model of the bladed rail structure. (b) Normalized resonance frequencies of the bladed assemblies (ω_1 is the first bending mode frequency of the first family)

of the system, the optimal location of the piezoelectric patches and the design of controller. In Section 3, experimental results are presented. The conclusions are drawn in Section 4.

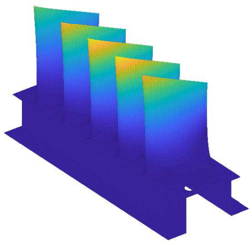

(a) Mode1

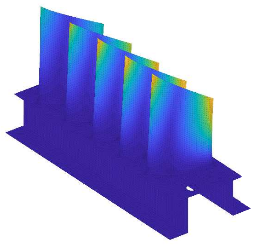

(b) Mode6

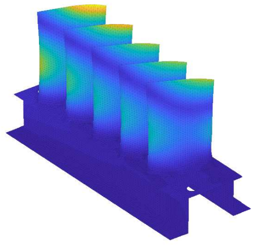

(c) Mode12

Figure 3: First mode shape of the (a) first, (b) second, and (c) third families

2 Numerical modeling of the bladed rail

Figure 1 shows the manufactured bladed rail which was made of aluminium. The monobloc bladed rail comprises five identical blades placed on a support. Its geometry is adapted to that of the conventional compressor bladed drum (BluM) [21]. As a boundary condition, the bottom part of the structure is clamped to a rigid wall. Due to the complexity of the structure, its finite-element-model (FEM), shown in Figure 2a, was built using shell elements. The normalized frequencies of the first seventeen modes of the structure are shown in Figure 2b. Note that the frequencies are normalized with respect to the frequency of the first resonance. Clearly, modes can be categorized into two types. The first type corresponds to the mode family consisting of five resonances with very close frequencies. Figure 3 shows the first mode shapes of the first three families. One sees that the motion of the blades are dominant such that the mode shapes of the first, second and third families are representing the first bending, the first torsion and the second bending of the blades, respectively. Note that the separation of the resonance frequencies in a family depends on the rigidity of the support. In addition, the second type of modes represent the resonances of the support which are isolated from others. In this study, the vibration of the first family of modes is of interest.

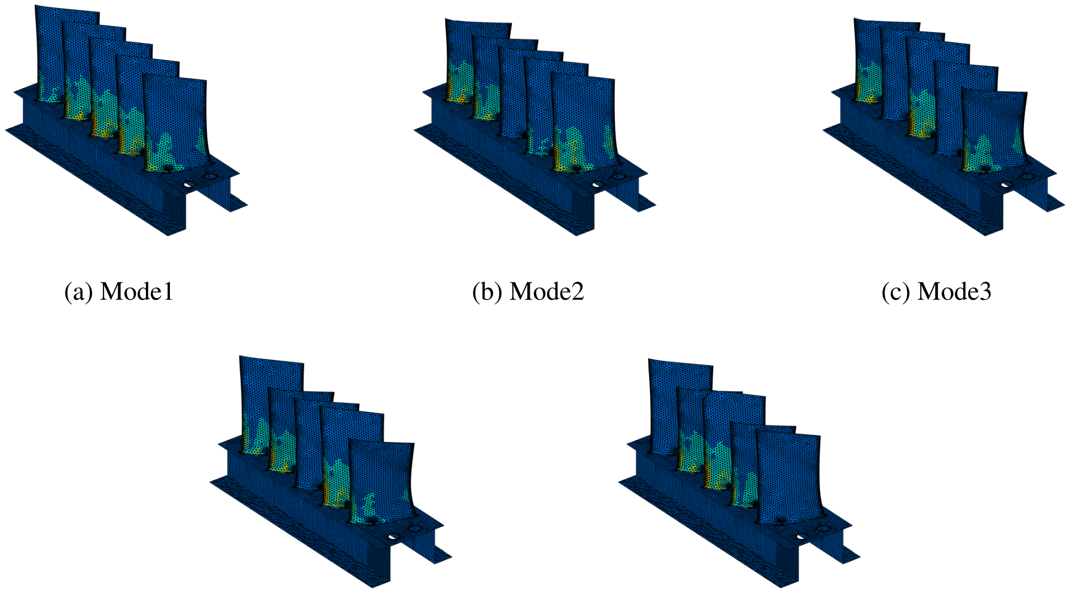

(a) Mode1 (b) Mode2 (c) Mode3

(d) Mode4 (e) Mode5

Figure 4: Strain energy distribution of the first five modes corresponding to the first family

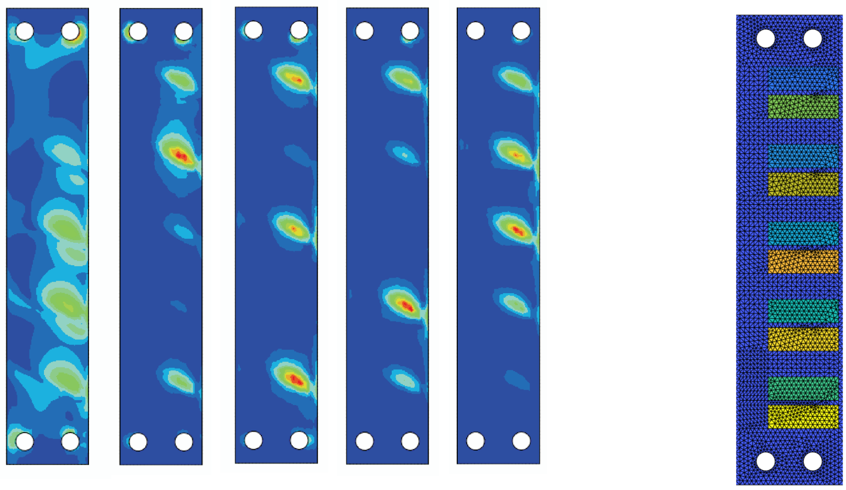

Mode1 Mode2 Mode3 Mode4 Mode5

(a)

(b)

Figure 5: (a) Strain distribution of the internal part of the support for the first family of modes. (b) Configuration of the piezoelectric patches on the structure

2.1 Optimal location of piezoelectric patches

Piezoelectric devices transform mechanical energy into electrical energy and vice versa. This property allows us to use the transducers as either sensors and/or actuators. When a piezoelectric patch is used as a sensor, the output voltage is proportional to the relative rotation of its extremities. Similarly, the moment applied by a piezoelectric patch is proportional to the relative rotation of its extremities. To maximize the observability and controlability, the optimal location of these transducers is the area of the structure where the strain energy is maximized. The strain energy map of the first five modes corresponding to the first family of modes is shown in Figure 4. One sees that the strain energy is maximized at the root of each blades. However, the patches cannot be placed there because they can easily disturb the aerodynamic flow. To overcome the aforementioned limitation, it is required to place the transducers on the internal part of the support. For this area, the strain map is shown in Figure 5a. It is clearly visible that a local strain distribution is generated below each blade. The local deformations are separated by an artificial nodal line where no strain is generated. Depending on the motion of a blade, the deformation is either in tension or in compression; and subsequently, the charge generated in a piezoelectric patch is either positive or negative. In order to avoid charge cancellation in the patches, the size of piezoelectric patches can not be greater than the local deformation area.

Assuming that the relative rotation of the extremities of both sensor and actuator is almost the same when they are placed next to each other, the frequency response function (FRF) from voltage applied by the actuator to the voltage measured by the sensor contains alternating pole-zero, i.e. collocated system, which is of interest in active control techniques since its phase is always between -180° and 180°. Consequently, two collocated piezoelectric patches (using one of them as sensor and the other one as an actuator) are placed on the support below each blade such that they cover local strain distribution as it can be seen in Figure 5b.

2.2 Control design

The open-loop transfer function from each piezoelectric actuator to its collocated piezoelectric sensor is shown in Figure 6. One sees that the system contains alternating zero-pole configuration with no high frequency roll-off. For each mode, the frequency of the pole is the same for all pairs because it corresponds to a resonance frequency of the blades, while the frequency of the zero changes. In an active control system, the controllability of a target resonance can be assessed by the distance between the frequency of the pole and the frequency of the zero. For example, the third pair is not efficient enough to damp the second resonance due to the close location of second zero with respect to the second pole. It is also similar for the fourth resonance too. However, this pair can highly add damping to the first, third and fifth resonances.

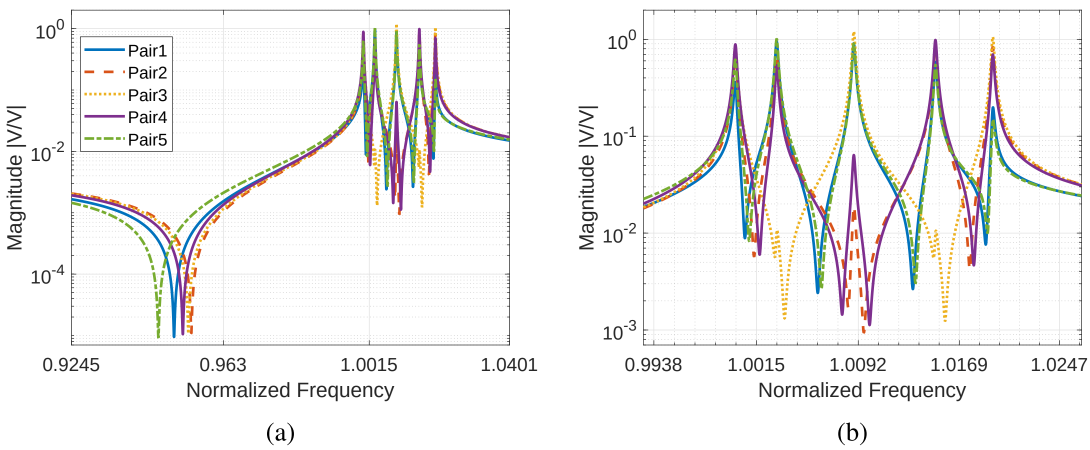

Figure 6: (a) FRF of the open-loop transfer function from each piezoelectric actuator to its collocated piezoelectric sensor. (b) Zoom close to the resonances.

The control configuration is shown in Figure 7, which is a multi-input-multi-output (MIMO) system with decentralized control system using the same control law. The choice of the control law is dependent on the location of zeroes with respect to poles. When the zeroes appear before poles, the open-loop transfer function is similar to that of a system when a force actuator is collocated to a force sensor. For such a system, two active control laws, including a simple integrator, known as integral-feedback (IF), or a double integrator combined with a real zero, known as α-controller, were proposed. Therefore, these two control laws are implemented in the present system as shown below:

$$H(s) = \frac{g_i}{s} \tag{1}$$

$$H(s) = \frac{g_{ii}(s+\alpha)}{s^2} \tag{2}$$

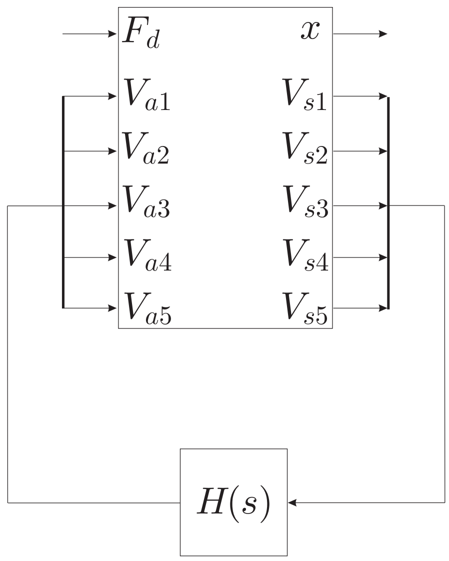

Figure 7: Block diagram of the numerical controller architecture.

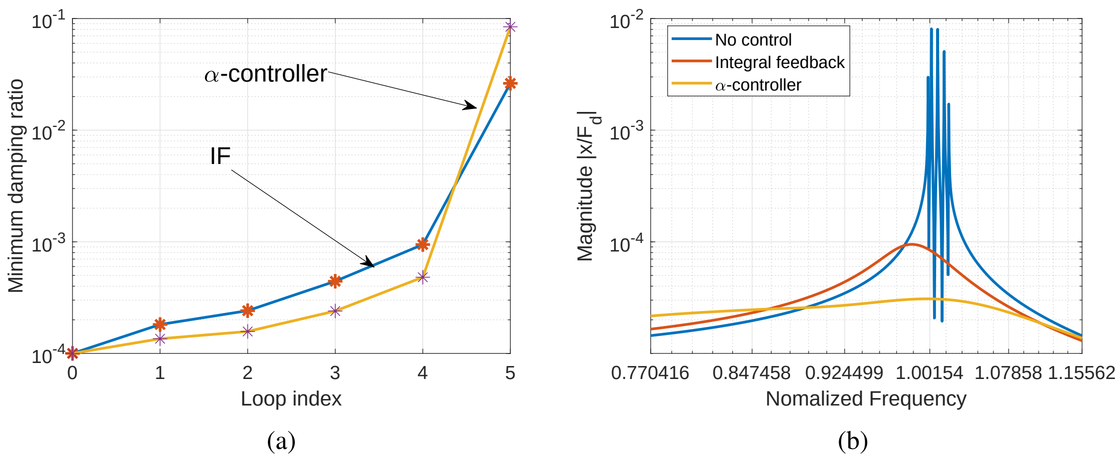

Figure 8: (a) Minimum damping ratio of the system against the number of closed loops. (b) Numerical FRF of the performance index with and without control system.

In order to tune the control parameters, a numerical optimization in MATLAB is employed using *fminsearch* function. The optimization consists in maximizing the minimum damping of the system. Figure 8a shows the minimum damping ratio of the first family of modes against the number of the closed-loops. As it can be seen when all the loops are closed, the minimum damping of the system is about 2.5% and 8% when the IF or α-controller is used, respectively. To check how effective the control system is, the performance index of the system is defined as the transfer function from the force injected at a tip of the fifth blade to the displacement at the same location. The FRF of the performance index with and without control systems is shown in Figure 8b. It can be clearly seen that the maximum amplitude of response when α-controller is used is three times lower than that of IF controller. Better control performance obtained by α-controller comes at the expense of a decrease in the phase margin. This can be seen in Figure 9 where the phase margin is plotted against the number of the closed-loop system. Note that the system is assumed to be multi-single-input-single-output (multi-SISO).

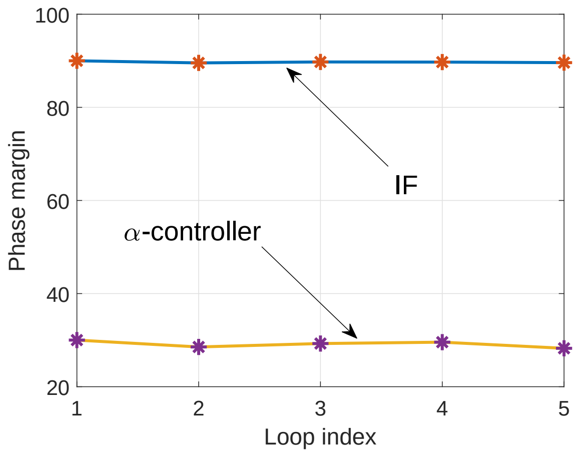

Figure 9: Phase margin against the number of closed-loops.

3 Experimental verification

To perform the experimental tests, a dSPACE MicroLabBox was used for the purpose of both the data acquisition and the control system. The control configuration is designed first inside the graphical SIMULINK environment of MATLAB and then compiled. The compiled file is uploaded into the ControlDesk software connected directly to the MicroLabBox hardware. The system is running in real time at a sampling frequency of 20 kHz. The measured data were recorded at the same sampling frequency.

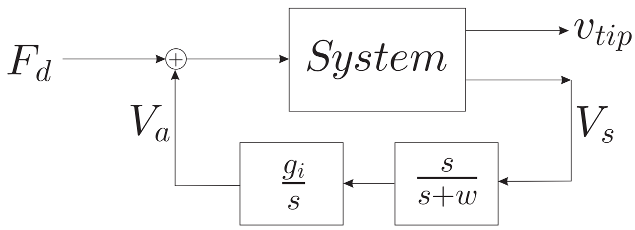

Figure 10: Block diagram of the experimental controller architecture.

In this study, the experiments were performed using only the fourth pair of patches. The configuration scheme for the experimental study is shown in Figure 10. F_d and V_a are the disturbance force and the actuation control voltage, respectively. Note that the same piezoelectric actuator was used for the excitation. A chirp signal generator excited the structure around the first family of resonances. v_{tip} and V_s are the tip velocity of the fifth blade and the voltage measured by the fourth piezoelectric patch, respectively. The velocity of the tip blade v_{tip} was measured by the polytec laser vibrometer. Therefore, the performance index is defined as the transfer function from the disturbance force F_d to the velocity of the tip blade v_{tip}.

The FRF of the experimental open-loop transfer function from the fourth piezoelectric patch to the fourth piezoelectric sensor is shown in Figure 11a. In order to further design the control system, a curve is fitted to the experimental FRF as it can be seen by red-dotted line. The obtained modal damping of the these resonances is 0.5%, 0.062%, 0.055%, 0.05% and 0.045% for the first, second, third, fourth and fifth modes, respectively. One sees that the first and fourth resonances do not clearly appear in the FRF. This is because the fourth blade does not almost move at the first and fourth resonance frequencies. Therefore, almost no strain is generated at the location of the piezoelectric patches.

In this study, we only focus on the implementation of an integral feedback. In order to avoid integrating the low-frequency contents of the sensor, a high-pass filter is also added in the feedback loop. The optimal value of the feedback gain is tuned following the procedure explained in the previous section. Figure 11b shows the loop gain of the system with optimal IF. 90° phase margin ensures the stability of the closed-loop system.

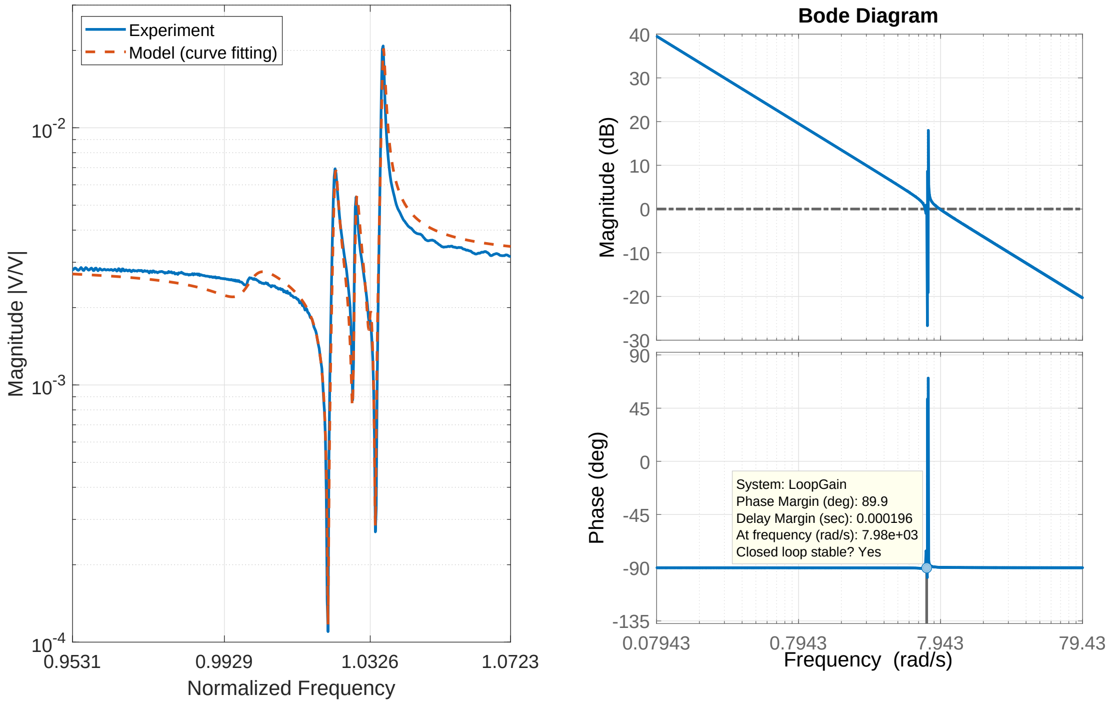

(a) (b)

Figure 11: (a) Experimental FRF of the open-loop transfer function from the fourth piezoelectric patch to the fourth piezoelectric sensor. (b) Loop-gain of the system with the application of IF.

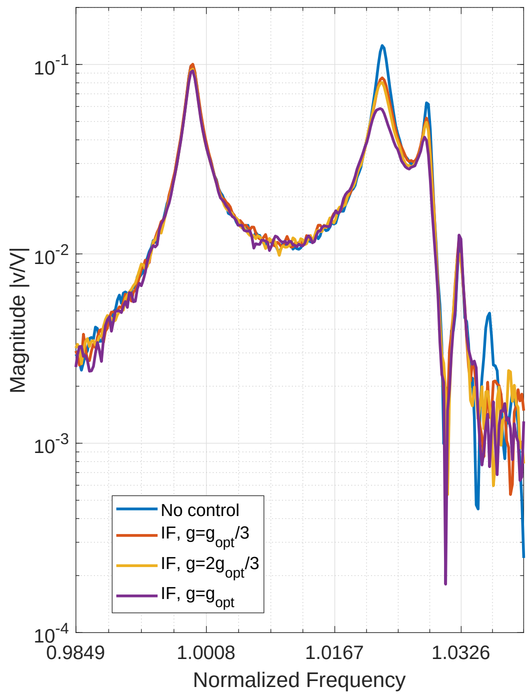

Figure 12: Experimental FRF of the performance index with and without control system.

The FRF of the experimental performance index from the disturbance force to the velocity of the tip fifth blade is presented in Figure 12. All resonances of the first family are visible. It can be seen that, the controller can damp the second, third and fifth resonance while it has no control over the first and fourth resonances as it was expected.

The experimental implementation of IF and the α-controller using all pairs of the patches is left for future work.

4 Conclusions

This paper proposed two active vibration damping techniques to damp the high modal density resonances of a bladed rail structure. The control laws were inspired by the force-feedback control system due to the similar pole-zero pattern in the open-loop transfer function. Piezoelectric patches were used for the implementation of the control system. The optimal placement of the piezoelectric patches was also investigated. It has been shown that locating the patches at the blade root maximizes the strain energy; however, it results in important perturbations of the aerodynamic flow. Therefore, a pair of sensor and actuator is placed inside the structure below each blades. The control systems were first designed numerically and then verified experimentally. The method of maximum damping which consists in maximizing the minimum damping of the first family of modes was used to optimize the parameters of the controller.

Acknowledgements

The authors are grateful to the financial support of MAVERIC (Wal'innov project 1610122).

References

[1] J. H. Griffin, "A review of friction damping of turbine blade vibration," *International Journal of Turbo and Jet Engines*, vol. 7, no. 3-4, pp. 297–308, 1990.

[2] D. Laxalde, C. Gibert, and F. Thouverez, "Experimental and numerical investigations of friction rings damping of blisks," in *Turbo Expo: Power for Land, Sea, and Air*, vol. 43154, 2008, pp. 469–479.

[3] D. Laxalde, F. Thouverez, and J.-P. Lombard, "Forced response analysis of integrally bladed disks with friction ring dampers," *Journal of Vibration and Acoustics*, vol. 132, no. 1, 2010.

[4] C. M. Firrone, M. Allara, and M. M. Gola, "A contact model for nonlinear forced response prediction of turbine blades: Calculation techniques and experimental comparison," in *Turbo Expo: Power for Land, Sea, and Air*, vol. 43154, 2008, pp. 573–582.

[5] S. M. Schwarzendahl, J. Szwedowicz, M. Neubauer, L. Panning, and J. Wallaschek, "On blade damping technology using passive piezoelectric dampers," in *Turbo Expo: Power for Land, Sea, and Air*, vol. 44731. American Society of Mechanical Engineers, 2012, pp. 1205–1215.

[6] B. Mokrani, R. Bastaits, M. Horodinca, I. Romanescu, I. Burda, R. Viguié, and A. Preumont, "Parallel piezoelectric shunt damping of rotationally periodic structures," *Advances in Materials Science and Engineering*, vol. 2015, 2015.

[7] J. Kauffman and G. Lesieutre, "Vibration reduction of turbomachinery bladed disks with changing dynamics using piezoelectric materials," in *52nd AIAA/ASME/ASCE/AHS/ASC Structures, Structural Dynamics and Materials Conference 19th AIAA/ASME/AHS Adaptive Structures Conference 13t*, 2011, p. 2003.

[8] A. Hohl, M. Neubauer, S. Schwarzendahl, L. Panning, and J. Wallaschek, "Active and semiactive vibration damping of turbine blades with piezoceramics," in *Active and Passive Smart Structures and Integrated Systems 2009*, vol. 7288. International Society for Optics and Photonics, 2009, p. 72881H.

[9] J. Tang and K. Wang, "Vibration control of rotationally periodic structures using passive piezoelectric shunt networks and active compensation," 1999.

[10] N. W. Hagood and A. von Flotow, "Damping of structural vibrations with piezoelectric materials and passive electrical networks," *Journal of sound and vibration*, vol. 146, no. 2, pp. 243–268, 1991.

[11] R. L. Forward, "Electromechanical transducer-coupled mechanical structure with negative capacitance compensation circuit," Jun. 19 1979, uS Patent 4,158,787.

[12] G. S. Agnes, "Active/passive piezoelectric vibration suppression," in *Smart Structures and Materials 1994: Passive Damping*, vol. 2193. International Society for Optics and Photonics, 1994, pp. 24–34.

[13] A. Preumont, *Vibration control of active structures: an introduction*. Springer, 2018, vol. 246.

[14] P. Remington, D. Sutliff, and S. Sommerfeldt, "Active control of low-speed fan tonal noise using actuators mounted in stator vanes: part 1 control system design and implementation," in *9th AIAA/CEAS Aeroacoustics Conference and Exhibit*, 2003, p. 3190.

[15] K. P. Duffy, B. B. Choi, A. J. Provenza, J. B. Min, and N. Kray, "Active piezoelectric vibration control of subscale composite fan blades," *Journal of engineering for gas turbines and power*, vol. 135, no. 1, 2013.

[16] C. E. Cesnik, S. Shin, and M. L. Wilbur, "Dynamic response of active twist rotor blades," *Smart materials and structures*, vol. 10, no. 1, p. 62, 2001.

[17] A. Paknejad, G. Zhao, M. Osée, A. Deraemaeker, F. Robert, and C. Collette, "A novel design of positive position feedback controller based on maximum damping and h 2 optimization," *Journal of Vibration and Control*, p. 1077546319892755, 2020.

[18] G. Zhao, A. Paknejad, G. Raze, A. Deraemaeker, G. Kerschen, and C. Collette, "Nonlinear positive position feedback control for mitigation of nonlinear vibrations," *Mechanical Systems and Signal Processing*, vol. 132, pp. 457–470, 2019.

[19] A. Preumont, J.-P. Dufour, and C. Malekian, "Active damping by a local force feedback with piezoelectric actuators," *Journal of guidance, control, and dynamics*, vol. 15, no. 2, pp. 390–395, 1992.

[20] S. Chesné, A. Milhomem, and C. Collette, "Enhanced damping of flexible structures using force feedback," *Journal of Guidance, Control, and Dynamics*, vol. 39, no. 7, pp. 1654–1658, 2016.

[21] B. Mokrani, R. Bastaits, M. Horodinca, I. Romanescu, I. Burda, R. Viguié, and A. Preumont, "Parallel piezoelectric shunt damping of rotationally periodic structures," *Advances in Materials Science and Engineering*, vol. 2015, 2015.